


Single-molecule localization microscopy goes quantitative

Silvia Scalisi^{1,2} | Dario Pisignano³ | Francesca Cella Zancchi^{2,3} 

¹Department of Cellular, Computational and Integrative Biology (CIBIO), University of Trento, Trento, Italy

²Nanoscopy and NIC@IIT, Istituto Italiano di Tecnologia, Genoa, Italy

³Dipartimento di Fisica “E. Fermi”, Università di Pisa, Pisa, Italy

Correspondence

Francesca Cella Zancchi, Dipartimento di Fisica “E. Fermi”, Università di Pisa, Largo B. Pontecorvo 3, Pisa, Italy.

Email: francesca.cella@unipi.it

Review Editor: Alberto Diaspro

Abstract

In the last few years, single-molecule localization (SMLM) techniques have been used to address biological questions in different research fields. More recently, super-resolution has also been proposed as a quantitative tool for quantifying protein copy numbers at the nanoscale level. In this scenario, quantitative approaches, mainly based on *stepwise photobleaching* and *quantitative SMLM* assisted by calibration standards, offer an exquisite tool for investigating protein complexes. This primer focuses on the basic concepts behind quantitative super-resolution microscopy, also providing strategies to overcome the technical hurdles that could limit their application.

KEYWORDS

fluorescence microscopy, quantitative stochastic optical reconstruction microscopy (STORM), single-molecule localization, super-resolution microscopy

Research Highlights

Super-resolution microscopy offers an exquisite tool to quantitatively study protein distribution in cellular systems. We highlight the main trends in quantitative super-resolution providing a simple guide to design quantitative experiments by single molecule localization microscopy.

1 | SUPER-RESOLUTION BY SINGLE-MOLECULE LOCALIZATION FLUORESCENCE MICROSCOPY

The spatial resolution of far-field optical microscopy is intrinsically limited by diffraction, and the resolution limit imposed by Abbe's law seemed impossible to overcome for a long time. During the last decades, many efforts have been made to bypass the “diffraction barrier,” overcoming the diffraction limit (Hell, 2007). Super-resolution microscopy, for which the Nobel Prize in Chemistry was awarded in 2014, circumvents the resolution limit and allows microscopy to glimpse into the vast world at the nanoscale, otherwise previously “invisible” to the eyes of optical fluorescence microscopes. Several techniques have been developed involving different concepts, according to which they can be grouped into two leading families: targeted readout-based and stochastic approaches (Diaspro & Bianchini, 2020; Hell, 2007; Sigal et al., 2018). The targeted readout triggers

photophysical transitions to “dark” transient states to shape the Point Spread Function (PSF) for resolution improvement. Conversely, the stochastic approach, to which single-molecule localization microscopies (SMLMs) (Endesfelder & Heilemann, 2014; Lelek et al., 2021; Möckl & Moerner, 2020) belong, exploits photophysical transitions of fluorophores to observe single molecules by separating them temporally and locating their position with nanometric precision (Deschout, Zancchi, et al., 2014; Endesfelder et al., 2014). In fact, the centroid position of a detected molecule is fitted, usually with a Gaussian distribution, and localized with a precision (Figure 1a) that scales with the number of detected photons. Scattered subsets of molecules are localized. Subsequently, the photophysical properties of the fluorophores enable the previously localized molecules to shift into a “dark” state and proceed to the localization of further subsets of molecules. The iteration of this process (Figure 1b) leads to reconstructing a map of molecule coordinates that provides an image containing sub-resolved information (Figure 1c). The single-molecule localization

This is an open access article under the terms of the [Creative Commons Attribution-NonCommercial](https://creativecommons.org/licenses/by-nc/4.0/) License, which permits use, distribution and reproduction in any medium, provided the original work is properly cited and is not used for commercial purposes.

© 2023 The Authors. *Microscopy Research and Technique* published by Wiley Periodicals LLC.

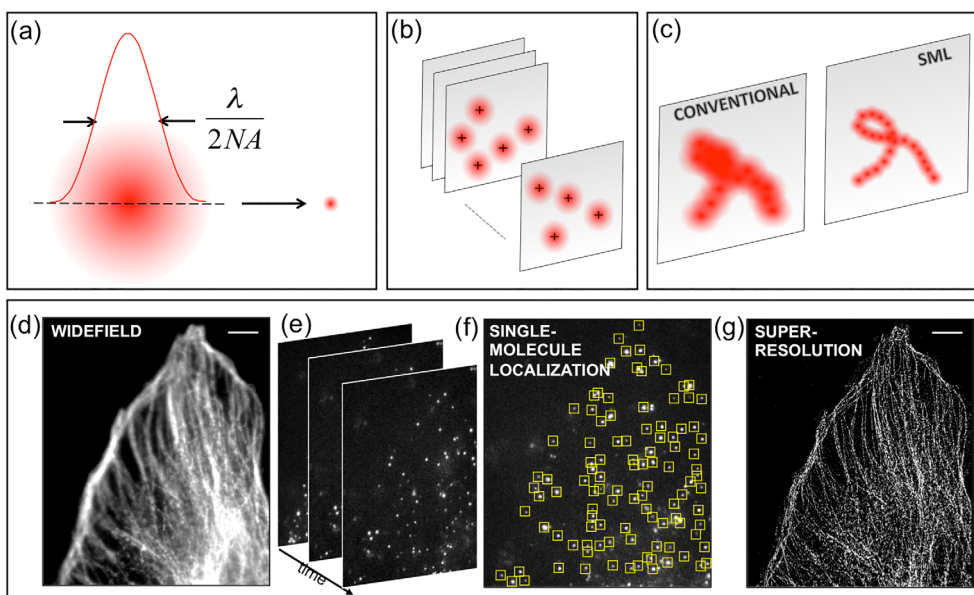


FIGURE 1 Single molecule localization microscopy. The localization concept (a); sequential acquisition and localization of sparse emitters (b) schematic representation of the resolution improvement provided by single-molecule localization compared to conventional microscopy (c) (Diaspro & Bianchini, 2020; Magrassi et al., 2019). Super-resolution imaging of alfa-tubulin in mammalian cells (d–g). Wide-field imaging of microtubules (d) and repeated imaging (e) of sparse emitters' subsets using a wide-field optical architecture. Each molecule is then identified setting a proper threshold and localized (f) with high precision for final super-resolution image reconstruction (g). Scale bars = 5 μm

concept is illustrated by imaging microtubules filaments in mammalian cells as an example. A strong resolution improvement is obtained compared to widefield imaging (Figure 1d). Sparse subsets of molecules are repeatedly imaged (Figure 1e) using a wide-field optical scheme and each molecule is then identified setting a proper threshold and localized with high precision (Figure 1f). When a sufficient number of molecules is collected, the map of their position is used to reconstruct a super-resolution image containing sub-diffraction features (Figure 1g).

The position of each molecule is calculated by the mean of the positions of each detected photon, and the localization precision (Thompson et al., 2002) may be expressed as the statistical error:

$$\sigma = \sqrt{\frac{s^2}{N}},$$

where, s is the width of the PSF of the system, and N is the number of collected photons. Considering the contribution due to the pixelation effect, the localization precision may be rewritten as:

$$\sigma = \sqrt{\frac{s^2}{N} + \frac{a^2}{12N}},$$

where, a is the pixel size. Finally, the additional contribution due to the background noise provides the following analytical and expression for the localization precision (Mortensen et al., 2010; Thompson et al., 2010):

$$\sigma = \sqrt{\frac{s^2}{N} + \frac{a^2}{12N} + \frac{4\sqrt{\pi}s^3b^2}{aN^2}},$$

where, b is the background noise.

The various well-established SMLM techniques differ mainly in the photo-physical phenomena exploited to induce the transition from the “on” state to the “off” state of the fluorescent probes. In fact, although the basic concept behind all the SMLMs is the same, PALM (photo-activated localization microscopy) uses fluorescent proteins (FPs) (Betzig et al., 2006; Hess et al., 2006), STORM (stochastic optical reconstruction microscopy) traditionally exploits organic dyes (Heilemann et al., 2008; Rust et al., 2006), while PAINT (point accumulation for imaging in nanoscale topography) (Jungmann et al., 2010; Sharonov & Hochstrasser, 2006) employs short complementary oligos (Schnitzbauer et al., 2017). Furthermore, the newly developed Minimal fluorescence photon fluxes (Balzarotti et al., 2017) (MINIFLUX) offers an innovative localization approach with improved nanometric localization capabilities (Ostersehl et al., 2022). Besides the nanoscale resolving ability of these state-of-art techniques, their power also relies on the advanced methods that can be implemented. Among the main current trends (Möckl & Moerner, 2020) in advanced single-molecule localization microscopy one should mention extending their capabilities to molecular counting and extending their imaging depth capabilities to thicker samples. Pushing the quantitative features of SMLMs (Deschout, Shivanandan, et al., 2014; Wu et al., 2020) would provide an exquisite tool for studying oligomeric states, the supra-molecular organization of macromolecular complexes and the clustering level of proteins in biological systems. On the other side, the development of optical schemes, extending the imaging depth by minimizing image degradation due to absorption and scattering effects, would provide the unique opportunity to peer into tissues and whole organisms with super-resolution imaging. Although the concept behind SMLMs may appear very simple, these techniques present several challenges from an experimental point of view. This primer

mainly focuses on the aspects needed to make single-molecule techniques practical for quantitative studies, with particular attention to STORM methods.

1.1 | Experimental requirements for STORM imaging

Single-molecule localization microscopy in principle requires relatively simple equipment (Figure 2):

- A high quality inverted wide-field microscope with highly inclined illumination and *total internal reflection fluorescence* (TIRF) (Fish, 2009). Different illumination schemes might be employed to achieve the best signal-to-noise ratio, reducing the background and thus improving the localization precision. In fact, in TIRF the exponentially decaying evanescent field close to the coverslip provides selected excitation within a very thin layer (100 nm), and most of the background signal is suppressed. Conversely in highly inclined illumination the light is shifted in the back focal plane of the objective lens, and illumination gets out from the objective at a narrow angle, resulting in an inclined beam passing through the sample. For this reason TIRF illumination well fits the requirements of basal membrane imaging, while inclined illumination provides higher flexibility in 3D samples.
- High-quality objectives, with high numerical aperture and magnification to ensure efficient photon collection from each single emitter.
- Sample drift and instabilities due to temperature variations may degrade the imaging performances, especially when a high number of frames are collected over time. For this reason, an automatic focusing system to prevent the sample shift is mandatory for proper image reconstruction.
- Typical laser intensities in SMLM experiments range from 0.5 to 2 kW/cm². High power lasers ensure optimal readout intensities for efficient blinking and molecule detection.
- The detector also plays a relevant role. Charge-coupled device (CCD) cameras are usually employed for single-molecule detection. Both

emCCDs and the new generation of CMOS cameras exhibit good sensitivity and performances. Which one may be preferable is often a personal choice since they differ for brightness and field of view, but it is not universally recognized whether one is preferable over the other.

1.2 | Factors limiting performance in localization microscopy

Different factors may impair the single-molecule localization ability, and a few experimental procedures have to be considered to minimize their impact.

- *Labeling density.* An optimal localization precision is not sufficient to achieve optimal resolution itself. In fact, the labeling efficiency plays a relevant role since it co-determines the spatial resolution by tuning the degree of decoration of the target molecules with fluorophores. Although the resolution correlates with the localization precision, image degradation occurs when fluorescent labeling fails to properly tag all the molecules of interest. Both a partial labeling efficiency and the loss of fluorescence of the tagged molecules (due to incomplete FPs maturation or fluorescence quenching) lead to a loss of content in the reconstructed super-resolution images. The spatial resolution may be defined considering that features smaller than twice the distance of two adjacent fluorophores cannot be reliably distinguished (Dempsey et al., 2011; Shroff et al., 2007). In this context, the *Nyquist criterion* provides a reliable guideline to define a sufficient labeling density to discriminate object closer than Δ :

$$\Delta = \frac{2}{\rho^{1/D}},$$

where, D is the dimension of the imaged structures and ρ is the emitter density.

- *Fluorescent probe.* The labeling strategy and the size of the fluorophores have a strong impact on SMLM performance and

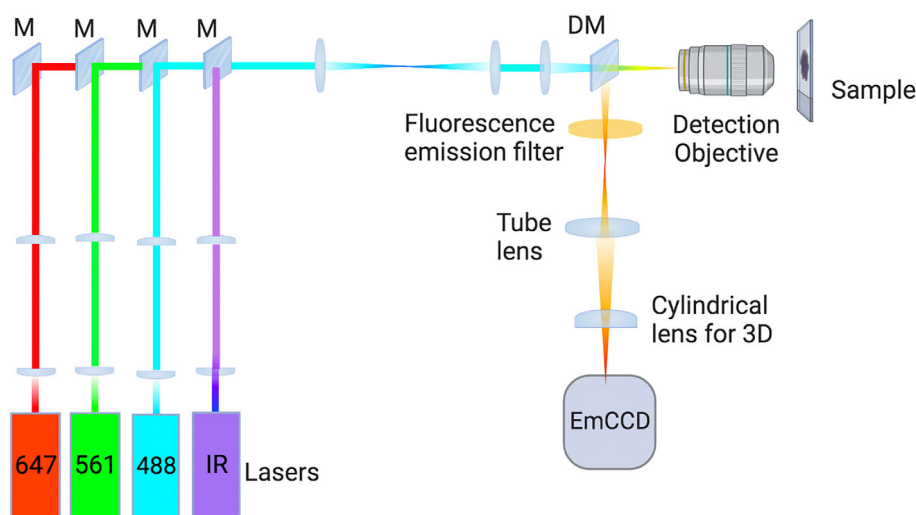


FIGURE 2 Wide-field based optical scheme for single-molecule localization microscopy. The system is equipped with four laser lines for activation and excitation and a high numerical aperture objective lens (100 \times NA = 1.49). Mirrors (M), dichroic mirrors (DM) and a band pass filters select illumination and fluorescence emission light. A cylindrical lens introduces astigmatism for axial single-molecule localization.

resolution. Proper fluorophores (Kikuchi et al., 2022; Vogelsang et al., 2010) and labeling strategies have to be chosen depending upon the specific biological application requirements (Erdmann et al., 2019; Fernandez-Suarez & Ting, 2008; Moore & Legant, 2018). FPs are excellent for live experiments, and for stepwise photobleaching, whereas immunostaining techniques perform better for SMLM. In fact, the optimal photophysics (i.e., brightness and photoswitching rates) for single-molecule localization is found with photoswitchable dye pairs. On the other hand, Halo and SNAP tags are very small (Erdmann et al., 2019) and can reduce bias due to steric hindrance while maintaining the benefits in terms of live cell experiments.

- **Imaging buffer.** An imaging buffer is often used to enable the photoswitching mechanism when organic dyes are employed as emitters in SMLMs (Bates et al., 2007). It usually consists of a reducing agent and an oxygen scavenger. For most of the organic fluorophores that operate on light/chemistry-induced photoswitching, a transition into a triplet state occurs, following reduction into a long-lived radical state (rhodamines, carbocyanines) or a fully reduced state (oxazines) (van de Linde et al., 2011). Unfortunately, although different imaging buffers are available, each of them works better with some dyes with respect to others, making the choice of the most suitable buffer for multi-color imaging quite difficult.

2 | SINGLE-MOLECULE LOCALIZATION MICROSCOPY GOES QUANTITATIVE

SMLM is a potentially helpful tool for quantitative biological experiments. The power of these techniques relies not only on the high spatial resolution achievable, but also on the further possibility of directly accessing quantitative information on a molecular scale (Deschout, Shivanandan, et al., 2014; Jung et al., 2017). Being able to count molecules would be of enormous significance in many aspects of life science since many biological functions are linked to the amount and spatial distribution of specific proteins in specific cellular compartments. Such quantitative information would provide a valid push forward for a better understanding of the etiology of many pathologies or the functioning of different cellular processes (Jung et al., 2017; Unterauer & Jungmann, 2021). The quantitative information of interest includes the spatial distribution of proteins, their organization in nanostructures/nanoclusters as well as the molecular counting for the study of the oligomeric states involved. Two are the main available approaches for extracting quantitative information from single molecule datasets: *stepwise photobleaching* and *quantitative SMLM*.

2.1 | Stepwise photobleaching

The first quantitative approach is stepwise photobleaching (Ulbrich & Isacoff, 2007), a fluorescence-based method exploiting the irreversible bleaching of FPs due to long-lasting exposure of the sample to low

excitation intensities. FPs bleaching is stochastic, and molecules bleach independently of each other. Under these assumptions, the decay of the fluorescence intensity in well-defined steps reflects the number of subunits of the underlying molecular complex (Das et al., 2007; Durisic et al., 2012; Tsekouras et al., 2016; Ulbrich & Isacoff, 2007). Molecules are then identified measuring the intensity traces from single spot images (Figure 3a), and the photobleaching molecule probability provides a subsequent intensity drop, correlating with each photobleaching event. The molecular counting is then linked to the measured number of downward steps in the fluorescent intensity (Figure 3a).

In principle, if a one-to-one ratio between the fluorophores and the proteins of interest is assumed, the number of molecules corresponds to the number of intensity steps observed (Durisic et al., 2012, 2014; Leake et al., 2006; Nakajo et al., 2010; Ulbrich & Isacoff, 2007). This correspondence is valid, assuming that every subunit carries a fluorescent label. The counting accuracy is directly linked with the possibility of obtaining a 1:1 stoichiometry between fluorescent tags and proteins of interest. This ratio may be achieved by lowering the expression level to reduce over-expression when transient transfection with genetically encoded FPs is used. Otherwise, a 1:1 labeling stoichiometry may be ensured by the recently developed CRISPR/Cas9 procedure (Sander & Joung, 2014) for FP sequence insertion in the protein native sequence. With this approach, the expression level of the fluorescent fusion protein is close to the endogenous one (Sander & Joung, 2014). If the labeling stoichiometry is not controllable, fluorescence calibration methods can help to strengthen the accuracy of the counting. Both synthetic nanostructures and intracellular proteins can be used as calibration systems to optimize the quantitative analysis, reducing miscounting errors (Hummert et al., 2021) and automatizing the analysis (Danial et al., 2022). However, stepwise photobleaching presents some intrinsic limitations. Indeed this method performs well only for counting a low number of molecules since the likelihood of missed bleaching events increases with the number of counted proteins. Although several advances have been recently made in the SP analysis (Hummert et al., 2021), also using machine learning and Bayesian approaches (Bryan Iv et al., 2022; Hummer et al., 2016; Li & Yang, 2019), still the robustness is often limited to a finite number of steps. So, when the number of molecules increases, different approaches such as quantitative single-molecule localization microscopy (qSMLM) are required. A high signal-to-noise ratio is mandatory for efficient observation of an apparent step-like behavior of the fluorescence intensity. Therefore, optical illumination architectures such as TIRF and highly inclined and laminated optical sheet microscopy (Konopka & Bednarek, 2008; Tokunaga et al., 2008) is the more suitable optical configuration, able to reduce the out-of-focus contribution by reducing the background signal.

2.2 | Quantitative SMLM

In SMLMs, single-molecule localization events from photoswitchable fluorescent probes binding target proteins are exploited to

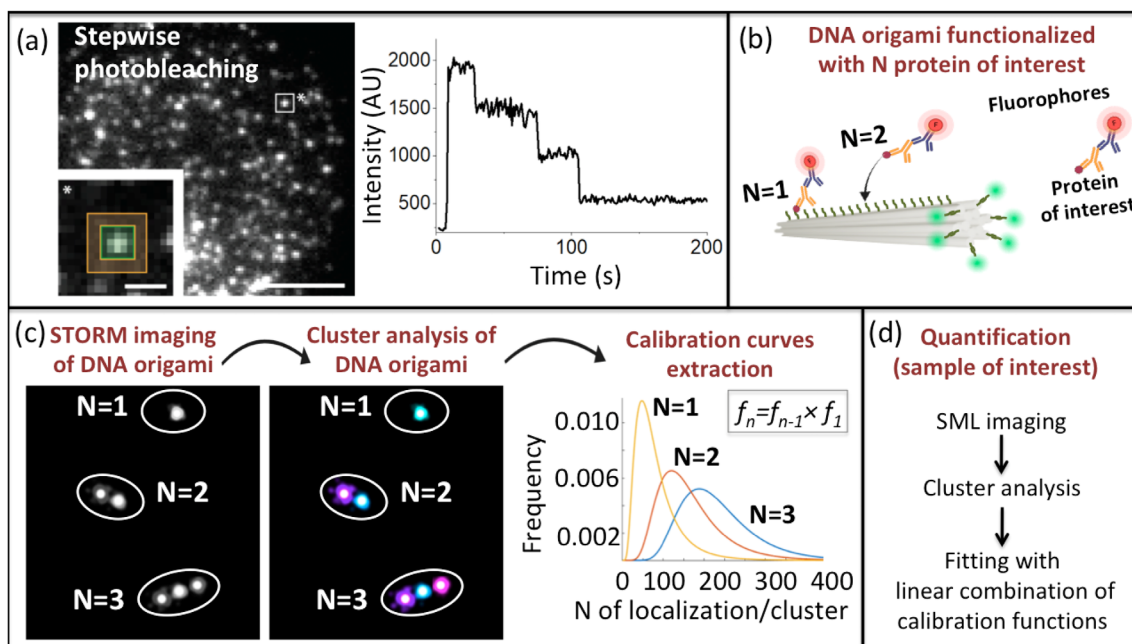


FIGURE 3 Quantitative single-molecule localization techniques. Imaging of separated membrane protein clusters (membrane proteins Barttin transfected with GFP) allows for stepwise photobleaching experiments (a). The effective number of fluorescent molecules may be estimated observing the drops in the intensity traces over time. Quantitative SMLM can be performed using DNA nanostructures (i.e., DNA origami) as calibration standards: Twelve-helix DNA origami chassis functionalized with a controlled number of proteins of interest (b). Calibration procedures (c) are based on STORM imaging, followed by cluster analysis, finalized to the extraction of a calibration curves dataset f_n . The pipeline (d) for absolute protein-copy number estimation follows three main steps: Single-molecule localization imaging, cluster analysis (under the same experimental conditions used for calibration) and fitting of the localizations histogram with a linear combination of calibration functions. Image modified from Cella Zancchi, Manzo, Alvarez, et al. (2017).

reconstruct images with a resolution of the order of 10–15 nm. Consequently, SMLM images already contain information about the number and spatial coordinates of molecules of interest (Dietz & Heilemann, 2019). Several analysis approaches have been developed to obtain quantitative information from SMLM datasets, studying the distribution and organization of the molecules at the nanoscale.

- **Cluster analysis.** SMLM datasets consist of a list of coordinates of single-molecules localized during the acquisition. In order to extract information about the spatial organization of these molecules, it is possible to apply cluster analysis (or clustering) to the output of SMLM (Khater et al., 2020; Nicovich et al., 2017). In general, the goal of cluster analysis is to group objects in clusters (i.e., groups) in which objects share more similarity with respect to those in different clusters. Besides life sciences, clustering algorithms are also applied nowadays to various fields. In SMLM, cluster analysis is employed to segment localization datasets, discerning among different topography and molecular organization. Protein clusters in different cell compartments are highly relevant in several functional mechanisms or pathologies. For example, a question of interest for membrane proteins studies is whether they are disassembled, clustered, or randomly distributed. Indeed, protein accumulation might reflect the formation of underlying membrane structure, or it can be a prerequisite for initiating some functional effect. In the last few years, several clustering algorithms

have been adapted, or newly developed, to analyze SMLM outputs (Khater et al., 2020; Nicovich et al., 2017). Algorithms based on the *nearest-neighbor index*, *Ripley's function*, and *pair-correlation function*, are derived from spatial statistics analysis tools (Clark & Evans, 1954; Owen et al., 2010; Ripley, 1977; Sengupta et al., 2011; Sengupta & Lippincott-Schwartz, 2012). These algorithms provide only an overall measure of clustering within a region of interest and average cluster size because they are limited to spatially homogeneous point processes, where the average density within the pattern is assumed to be independent of the spatial position. Other approaches must be considered if metrics per cluster are needed, such as cluster number, shape, or size. The *density-based analysis algorithms* process the localization data by exploiting the difference in density between the protein assemblies and the background. Clusters are considered a set of data objects spread over a contiguous region of high objects density and separated from each other by contiguous regions of low object density. One of the most popular density-based algorithms applied to SMLM data is the density-based spatial clustering of applications with noise, DBSCAN (Ester et al., 1996). DBSCAN considers two parameters for clustering: a neighborhood radius, ϵ , and a minimum number of points falling inside the radius to consider localizations as a cluster. However, it may fail when the cluster density range is wide (Nicovich et al., 2017). Another family of clustering algorithms is based on the generation of a mesh representation,

usually, a Voronoi diagram or a Delaunay triangulation, named *tessellation algorithms* (Andronov et al., 2018; Lvet et al., 2019). Basically, they consist of partitioning the molecular localization space into polygonal regions, each one centered around one of the molecules. The geometrical properties of the polygons depend on the spatial distribution and density of included points. The tessellation approach might fail the task when data show artifacts due to multiple blinking. Recently, graph-based (Pennacchietti et al., 2017) and machine-learning-based methods (Kosuta et al., 2020) have been developed to analyze SMLM datasets quantitatively.

- **Advanced quantitative SMLM methods.** In principle, the information hailing from localization datasets after cluster analysis may be directly linked with the exact number of proteins of interest. Still, the unpredictable stoichiometry of the labeling strongly impairs a linear conversion of SMLM datasets into protein numbers and requires additional strategies to mitigate such a limitation (Hummer et al., 2016). When immunostaining is performed, the number of fluorophores conjugated to the antibodies is highly stochastic. Moreover, fluorophores employed in SMLMs blink and their repeated reactivation events lead to overcounting. On the other hand, when fluorescent fusion proteins are used, both overcounting due to overexpression and undercounting given by incomplete FPs maturation may occur. Although optimized sample preparation procedures might minimize these effects, they can hardly be avoided. Despite CRISPR/Cas9 procedures offer a 1:1 labeling ratio and ensure a fusion protein expression close to the endogenous one, their significant cost might prevent their use on a routine base. For this reason, a way to overcome the hurdles in quantifying SMLM data using immunostaining and transient transfection with fluorescent FPs is to “calibrate” with structures featuring a known number of proteins. This way, precise conversion of the number of localizations per cluster into protein numbers can be obtained.

Several calibration methods have been recently proposed to quantify the accurate protein copy number distribution in an unknown biological sample. Calibration may be carried out by synthetic nanostructures (Cella Zanacchi et al., 2019; Cella Zanacchi, Manzo, Alvarez, et al., 2017; Jungmann et al., 2016; Scheckenbach et al., 2020) or monomeric/multimeric variants of known intracellular proteins/molecules (Danial et al., 2022; Finan et al., 2015; Fricke et al., 2015; Hummert et al., 2021; Thevathasan et al., 2019). Exploiting biological molecules as reference standards for counting is, in principle, preferable, since the calibration well reproduces the cellular environment. Still, most of these calibration proteins are monomeric, and it may fail accuracy when investigating molecules organized in more densely packed clusters. In this scenario, synthetic nanostructures—including DNA origami (Scheckenbach et al., 2020), patterns generated by cut-and-paste technology (SMCP) (Kufer et al., 2008) and DNA bricks (Ke et al., 2012)—provide flexibility mimicking different environments. In particular, DNA origami structures represent a valuable tool to calibrate, providing a versatile way to characterize at the single-molecule level the response from a given number of fluorophores

or proteins located at known positions. DNA origami can be immobilized on glass surfaces and can be used to characterize the photophysical behavior of a “single” dye or protein in terms of:

- a. Number of localizations/molecule.
- b. Fluorescence intensity.
- c. Blinking rate.
- d. Distances among proteins attached at specific handles.

STORM imaging combined with DNA origami as calibration standards may be used to quantify oligomeric states and molecular distribution of intracellular proteins (Cella Zanacchi, Manzo, Alvarez, et al., 2017). Furthermore, quantitative point accumulation in nano-scale topography (qPAINT) (Jungmann et al., 2016), where individual dye-labeled DNA strands transiently bind to target proteins functionalized with complementary strands, is an alternative approach for quantitative SMLM. The dye emits fluorescence only when the complementary strands are bound. It is then possible to extrapolate the number of proteins from the apparent blinking by extracting binding kinetics related to molecular numbers through basic kinetics equations (Jungmann et al., 2016). As an example, we will now focus on quantitative STORM protocols (Cella Zanacchi et al., 2019; Cella Zanacchi, Manzo, Alvarez, et al., 2017; Cella Zanacchi, Manzo, Sandoval Alvarez, et al., 2017) based on DNA origami calibration. qSTORM is performed in two main steps: calibration and quantification phases. The calibration is performed using 12-helix DNA origami structures, functionalized with N proteins of interest (Figure 3b), as a calibration tool. DNA origamis are also labeled with fluorescent reference markers (TAMRA) to facilitate nanostructure identification. Briefly, DNA origami with a controlled number of molecules are imaged by STORM. The localization datasets are then analyzed by cluster analysis (Figure 3c). The histograms of the localizations/cluster thus provide a set of calibration curves, f_n (Figure 3c). At this point, a second phase needs to compute the number of proteins contained in an “unknown” sample begins. The sample of interest is imaged by STORM under the same experimental conditions used for the DNA origami calibration imaging. The localizations/cluster histogram, hailing from the SMLM dataset and presumably containing a mixture of different oligomeric states, may be fitted to a linear combination of f_n functions (Figure 3d):

$$g(x) = \sum_{n=1}^{N_{\max}} \alpha_n f_n(x),$$

where, α_n represent the weights of the distribution of n -mers and:

$$\sum_{n=1}^{N_{\max}} \alpha_n = 1.$$

Fitting is performed by numerical minimization of the “objective function,” containing the sum of the entropy and the negative log-likelihood. The stop criterion for the fit is determined by minimizing the objective function that provides also the optimal number of functions used for the fit (N_{\max}). A detailed protocol, with further

information on qSTORM procedures, may be found in the literature (Cella Zanacchi, Manzo, Sandoval Alvarez, et al., 2017). Alternatively, other STORM methods rely on the analytical modeling of the fluorophore blinking statistics and might be used to access quantitative information. For simple kinetic models of photophysics, the resulting analytical formulas for the blinking statistics provide the basis for a model-independent (Hummer et al., 2016) and robust protein estimation (Möller et al., 2020).

3 | BIOLOGICAL APPLICATIONS

The quantitative tools described above smoothed the way for addressing several biological questions of interest. Different possible applications include the study of membrane proteins and accessory subunits (Nakajo et al., 2010; Ulbrich & Isacoff, 2007), synaptic proteins and receptors (Siddig & Aufmkolk, 2020), focal adhesion complexes (Scalisi et al., 2021), and other structures (Magrassi et al., 2019). Recent studies used stepwise photobleaching and revealed the oligomerization state of several GPCRs and the role of these oligomers in signaling (Milstein et al., 2022; Möller et al., 2020). For example, stepwise photobleaching (Figure 4a) showed the tetrameric form of the voltage-gated potassium channel KCNQ1 (Figure 4b). Furthermore, quantitative dSTORM characterized the nanoscale organization of the mGluR4 receptors (Figure 4c) within active zones at the presynaptic sites, showing multiple nano-domains, each containing either monomers, dimers or oligomers (Figure 4d).

4 | SINGLE-MOLECULE GOES DEEPER

SMLM microscopy has proven its capability to elucidate details and provide insights with unprecedented resolution into the world of biological processes. However, most studies are currently carried out at the cell culture level. Unfortunately, 2D cultures are surrounded by a modified environment and cannot correctly mimic the physiological conditions of living organisms. For this reason, the cell biology community needs to move from 2D cell cultures to three-dimensional tissue models (*Nature Methods*, 2018) and whole organisms. In the current scenario, the dream is still represented by the ideal possibility of performing super-resolution imaging directly into tissues of living organisms. In this framework, the next essential step is to identify strategies for super-resolution microscopy 3D model systems relevant from the physiological point of view. In the last few years, super-resolution and model systems have significantly evolved. However, some challenges remain, and they should make further progress together for a perfect match.

For single-molecule localization microscopy, the key point is to minimize the light-sample interaction, reducing the scattering effects that can deteriorate super-resolution performances in thick samples. Within this scenario, it is essential to identify the best illumination approach to minimize the background noise and thus improve the imaging depth. In fact, for better localization of individual emitters, a lot of attention has to be addressed to the reduction of the background b , since it can affect the localization precision:

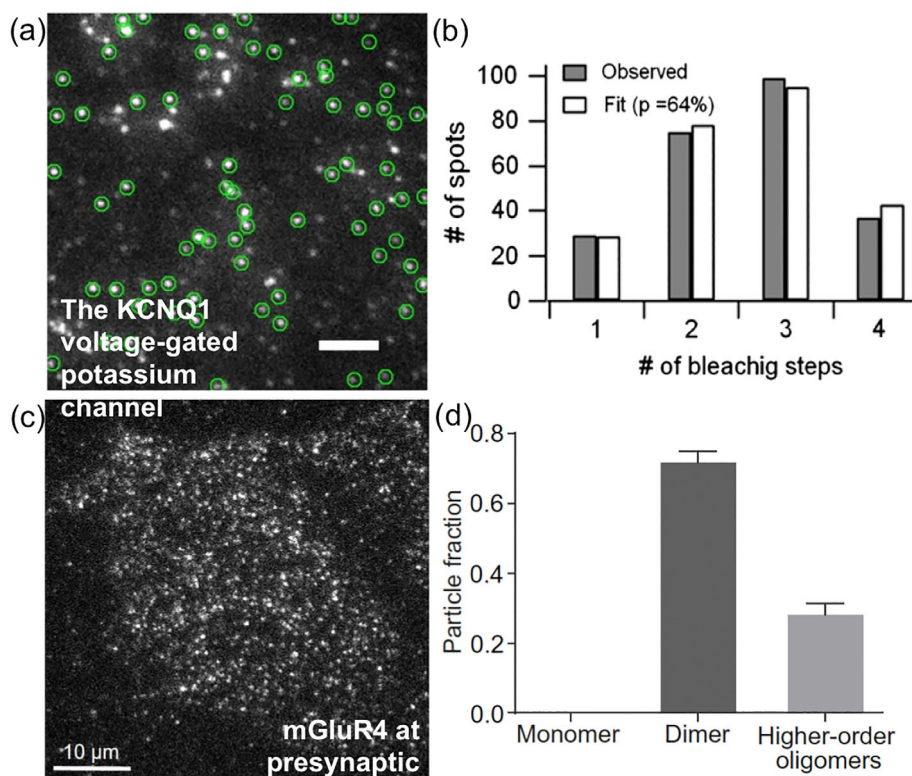
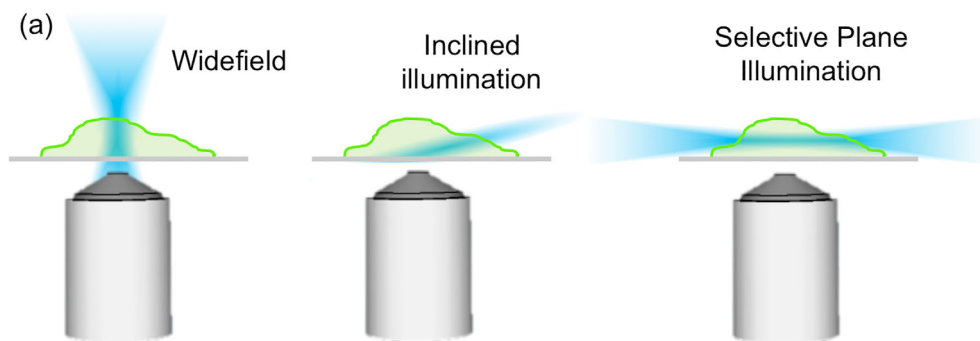


FIGURE 4 Application of stepwise photo-bleaching and qSMLM. KCNQ1 images from oocytes expressing mEGFP-KCNQ1 (a). Distributions of the observed bleaching steps (gray) and corresponding fit by a binomial distribution (white). qSMLM show the nanoscale organization of glutamate receptors mGluR4 (c) containing a fraction of either monomers, dimers and higher order oligomers (d) at presynaptic active zones. Image modified from Nakajo et al. (2010) and Siddig and Aufmkolk (2020), respectively

FIGURE 5 Optical illumination schemes for 3D single-molecule detection. Widefield illumination (a), oblique illumination (b), total internal reflection (c) and light-sheet microscopy (d)



$$\sigma_{x,y}^2 \approx \frac{s^2 + \frac{a^2}{12}}{N} + f(b, N^2),$$

where, s is the PSF width, a is related to the pixel size, N is the number of photons and b is the background noise. This relation shows that the uncertainty falls as the inverse of the number of photons for the background noise. Therefore, maximizing the number of photons collected for each molecule is crucial in SMLM imaging to increase localization precision. Furthermore, several factors limit the resolution for practical imaging of large scattering biological samples, mainly related to scattering and aberration effects. Additional errors induced in the localization process may affect the effective localization precision, and the overall precision is redefined by considering the additional instabilities of the system (ϑ_{inst}):

$$\sigma_{eff}^2 = \sqrt{2\sigma_{x,y}^2 + \sigma_{inst}^2},$$

where a factor 2 takes into account the excess noise (Aquino et al., 2011) introduced by the electron multiplying process of emCCDs. The choice of the optimal illumination scheme may play an essential role in background reduction and imaging depth improvement. Optical schemes based on TIRF and inclined illumination (Konopka & Bednarek, 2008; Tokunaga et al., 2008) are widely used for their ability to reduce the background and out of focus contributions. In fact a significant reduction of the background compared to widefield imaging (Figure 5a) can be gained axially confining the illumination process by highly inclined laminated microscopy (HILO) (Tokunaga et al., 2008) (Figure 5b) or TIRF-based microscopy (Fish, 2009) (Figure 5c).

In TIRFM the illumination beam illuminates the coverslip with an incident angle higher than the critical angle generating evanescent waves. The axial confinement of the excitation volume (50–150 nm deep into the sample) relies on the exponential decay in the proximity of the glass surface of the evanescent waves. Since the imaging depth into the specimen is limited to a few hundred nanometers (Figure 5c), TIRF application is still limited to studies of proteins near the basal cellular membrane. Inclined illumination (Figure 5b) is often implemented to overcome the substantial limitation of TIRF illumination on the axial depth. HILO microscopy illuminates the sample with an inclined light sheet and is a popular configuration for intracellular single-molecule imaging. However, the imaging depth remains basically

confined at the cellular level. Within this context, further evolution is represented by light-sheet microscopy (Figure 5d). In light sheet illumination, decoupling the illumination and the detection path (Huisken et al., 2004) allowed imaging with a low background within thick samples. Indeed, the light sheet approach freely moves the illumination within the sample, reducing the background signal coming from out-of-focus contributions. These features made this approach particularly promising for further application of super-resolution to thicker samples. Recently, optical configurations based on single objective (Galland et al., 2015), reflected (Greiss et al., 2016) and tilted (Gustavsson et al., 2018) light sheet illumination demonstrated 3D super-resolution imaging capabilities in thick cells or small organisms. For example, conventional selective plane illumination microscopy was proven to be a promising tool for further imaging depth improvement, demonstrating single-molecule imaging in multicellular spheroids up to 200 μm depths (Cella Znacchi et al., 2011, 2013). Nonetheless, super-resolution is still hardly feasible in more complicated tissues, where the scattering and absorption properties of the samples prevent single-molecule imaging. Despite the promising progress of light sheet microscopy, wide-field-based configurations (such as TIRF and HILO) remain the most popular modality implemented in imaging core facilities, due to the more straightforward optical implementation.

AUTHOR CONTRIBUTIONS

Silvia Scalisi: Writing – original draft; methodology. **Dario Pisignano:** Writing – review & editing; resources. **Francesca Cella Znacchi:** Conceptualization; methodology; writing – original draft; writing – review & editing; software; supervision.

ACKNOWLEDGMENT

We acknowledge the Nikon Imaging Center at Istituto Italiano di Tecnologia and the Center for Instrument Sharing at University of Pisa (CISUP).

CONFLICT OF INTEREST

The authors declare no conflict of interest.

DATA AVAILABILITY STATEMENT

The data that support the findings of this study are available from the corresponding author upon reasonable request.

ORCID

Francesca Cella Zancacchi  <https://orcid.org/0000-0002-2427-3009>

REFERENCES

- Andronov, L., Michalon, J., Ouararhni, K., Orlov, I., Hamiche, A., Vonesch, J. L., & Klaholz, B. P. (2018). 3DClusterViSu: 3D clustering analysis of super-resolution microscopy data by 3D Voronoi tessellations. *Bioinformatics*, *34*, 3004–3012. <https://doi.org/10.1093/bioinformatics/bty200>
- Aquino, D., Schönle, A., Geisler, C., Middendorff, C., Wurm, C. A., Okamura, Y., Lang, T., Hell, S. W., & Egnér, A. (2011). Two-color nanoscopy of three-dimensional volumes by 4Pi detection of stochastically switched fluorophores. *Nature Methods*, *8*, 353–359.
- Balzarotti, F., Eilers, Y., Gwosch, K. C., Gynnå, A. H., Westphal, V., Stefani, F. D., Elf, J., & Hell, S. W. (2017). Nanometer resolution imaging and tracking of fluorescent molecules with minimal photon fluxes. *Science*, *355*, 606–612. <https://doi.org/10.1126/science.aak9913>
- Bates, M., Huang, B., Dempsey, G. T., & Zhuang, X. (2007). Multicolor super-resolution imaging with photo-switchable fluorescent probes. *Science*, *317*, 1749–1753.
- Betzig, E., Patterson, G. H., Sougrat, R., Lindwasser, O. W., Olenych, S., Bonifacio, J. S., Davidson, M. W., Lippincott-Schwartz, J., & Hess, H. F. (2006). Imaging intracellular fluorescent proteins at nanometer resolution. *Science*, *313*, 1642–1645.
- Bryan Iv, J. S., Sgouralis, I., & Pressé, S. (2022). Diffraction-limited molecular cluster quantification with Bayesian nonparametrics. *Nature Computational Science*, *2*, 102–111. <https://doi.org/10.1038/s43588-022-00197-1>
- Cella Zancacchi, F., Lavagnino, Z., Faretta, M., Furia, L., & Diaspro, A. (2013). Light-sheet confined super-resolution using two-photon photoactivation. *PLoS One*, *8*, e67667.
- Cella Zancacchi, F., Lavagnino, Z., Perrone Donnorso, M., del Bue, A., Furia, L., Faretta, M., & Diaspro, A. (2011). Live-cell 3D super-resolution imaging in thick biological samples. *Nature Methods*, *8*, 1047–1049.
- Cella Zancacchi, F., Manzo, C., Alvarez, A., Derr, N., Parajo, M., & Lakadamyali, M. (2017). A DNA origami platform for quantifying protein copy number in super-resolution. *Nature Methods*, *14*, 789–792. <https://doi.org/10.1038/nmeth.4342>
- Cella Zancacchi, F., Manzo, C., Magrassi, R., Derr, N. D., & Lakadamyali, M. (2019). Quantifying protein copy number in super resolution using an imaging-invariant calibration. *Biophysical Journal*, *116*, 2195–2203. <https://doi.org/10.1016/j.bpj.2019.04.026>
- Cella Zancacchi, F., Manzo, C., Sandoval Alvarez, A., Derr, N. D., Garcia Parajo, M., & Lakadamyali, M. (2017). A protocol to quantify protein copy number in super-resolution using DNA origami as a calibration standard. *Protocol Exchange*. <https://doi.org/10.1038/protex.2017.089>
- Clark, P. J., & Evans, F. C. (1954). Distance to nearest neighbor as a measure of spatial relationships in populations. *Ecology*, *35*, 445–453. <https://doi.org/10.2307/1931034>
- Danial, J. S. H., Quintana, Y., Ros, U., Shalaby, R., Margheritis, E. G., Chumpen Ramirez, S., Ungermann, C., Garcia-Saez, A. J., & Cosentino, K. (2022). Systematic assessment of the accuracy of subunit counting in biomolecular complexes using automated single-molecule brightness analysis. *The Journal of Physical Chemistry Letters*, *13*, 822–829. <https://doi.org/10.1021/acs.jpcl.1c03835>
- Das, S. K., Darshi, M., Cheley, S., Wallace, M. I., & Bayley, H. (2007). Membrane protein stoichiometry determined from the step-wise photo-bleaching of dye-labelled subunits. *ChemBiochem*, *8*, 994–999. <https://doi.org/10.1002/cbic.200600474>
- Dempsey, G. T., Vaughan, J. C., Chen, K. H., Bates, M., & Zhuang, X. (2011). Evaluation of fluorophores for optimal performance in localization-based super-resolution imaging. *Nature Methods*, *8*, 1027–1036. <https://doi.org/10.1038/nmeth.1768>
- Deschout, H., Shivanandan, A., Annibale, P., Scarselli, M., & Radenovic, A. (2014). Progress in quantitative single-molecule localization microscopy. *Histochemistry and Cell Biology*, *142*, 5–17. <https://doi.org/10.1007/s00418-014-1217-y>
- Deschout, H., Zancacchi, F. C., Mlodzianoski, M., Diaspro, A., Bewersdorf, J., Hess, S. T., & Braeckmans, K. (2014). Precisely and accurately localizing single emitters in fluorescence microscopy. *Nature Methods*, *11*, 253–266. <https://doi.org/10.1038/nmeth.2843>
- Diaspro, A., & Bianchini, P. (2020). Optical nanoscopy. *La Rivista del Nuovo Cimento*, *43*, 385–455. <https://doi.org/10.1007/s40766-020-00008-1>
- Dietz, M. S., & Heilemann, M. (2019). Optical super-resolution microscopy unravels the molecular composition of functional protein complexes. *Nanoscale*, *11*, 17981–17991. <https://doi.org/10.1039/C9NR06364A>
- Duriscic, N., Godin, A. G., Wever, C. M., Heyes, C. D., Lakadamyali, M., & Dent, J. A. (2012). Stoichiometry of the human glycine receptor revealed by direct subunit counting. *The Journal of Neuroscience: The Official Journal of the Society for Neuroscience*, *32*, 12915–12920. <https://doi.org/10.1523/JNEUROSCI.2050-12.2012>
- Duriscic, N., Laparra-Cuervo, L., Sandoval-Alvarez, A., Borbely, J. S., & Lakadamyali, M. (2014). Single-molecule evaluation of fluorescent protein photoactivation efficiency using an in vivo nanotemplate. *Nature Methods*, *11*, 156–162. <https://doi.org/10.1038/nmeth.2784>
- Endesfelder, U., & Heilemann, M. (2014). Art and artifacts in single-molecule localization microscopy: Beyond attractive images. *Nature Methods*, *11*, 235–238. <https://doi.org/10.1038/nmeth.2852>
- Endesfelder, U., Malkusch, S., Fricke, F., & Heilemann, M. (2014). A simple method to estimate the average localization precision of a single-molecule localization microscopy experiment. *Histochemistry and Cell Biology*, *141*, 629–638. <https://doi.org/10.1007/s00418-014-1192-3>
- Erdmann, R. S., Baguley, S. W., Richens, J. H., Wissner, R. F., Xi, Z., Allgeyer, E. S., Zhong, S., Thompson, A. D., Lowe, N., Butler, R., Bewersdorf, J., Rothman, J. E., St Johnston, D., Schepartz, A., & Toomre, D. (2019). Labeling strategies matter for super-resolution microscopy: A comparison between HaloTags and SNAP-tags. *Cell Chemical Biology*, *26*, 584–592.e586.
- Ester, M. K., Kriegel, H.-P., Sander, J., & Xu, X. (1996). A density based algorithm for discovering clusters in large spatial database with noise. In *Proceedings of 2nd international conference on knowledge discovery and data mining* (Vol. 34, pp. 226–231).
- Fernandez-Suarez, M., & Ting, A. Y. (2008). Fluorescent probes for super-resolution imaging in living cells. *Nature Reviews. Molecular Cell Biology*, *9*, 929–943. <https://doi.org/10.1038/nrm2531>
- Finan, K., Raulf, A., & Heilemann, M. (2015). A set of homo-oligomeric standards allows accurate protein counting. *Angewandte Chemie International Edition*, *54*, 12049–12052. <https://doi.org/10.1002/anie.201505664>
- Fish, K. N. (2009). Total internal reflection fluorescence (TIRF) microscopy. *Current Protocols in Cytometry*, *50*, 12.18.11–12.18.13. <https://doi.org/10.1002/0471142956.cy1218s50>
- Fricke, F., Beaudouin, J., Eils, R., & Heilemann, M. (2015). One, two or three? Probing the stoichiometry of membrane proteins by single-molecule localization microscopy. *Scientific Reports*, *5*, 14072. <https://doi.org/10.1038/srep14072>
- Galland, R., Greci, G., Aravind, A., Viasnoff, V., Studer, V., & Sibarita, J. B. (2015). 3D high- and super-resolution imaging using single-objective SPIM. *Nature Methods*, *12*, 641–644. <https://doi.org/10.1038/nmeth.3402>
- Greiss, F., Deligiannaki, M., Jung, C., Gaul, U., & Braun, D. (2016). Single-molecule imaging in living drosophila embryos with reflected light-sheet microscopy. *Biophysical Journal*, *110*, 939–946. <https://doi.org/10.1016/j.bpj.2015.12.035>
- Gustavsson, A. K., Petrov, P. N., Lee, M. Y., Shechtman, Y., & Moerner, W. E. (2018). 3D single-molecule super-resolution

- microscopy with a tilted light sheet. *Nature Communications*, 9, 123. <https://doi.org/10.1038/s41467-017-02563-4>
- Heilemann, M., van de Linde, S., Schüttelpe, M., Kasper, R., Seefeldt, B., Mukherjee, A., Tinnefeld, P., & Sauer, M. (2008). Subdiffraction-resolution fluorescence imaging with conventional fluorescent probes. *Angewandte Chemie (International Ed. in English)*, 47, 6172–6176. <https://doi.org/10.1002/anie.200802376>
- Hell, S. W. (2007). Far-field optical nanoscopy. *Science*, 316, 1153–1158.
- Hess, S. T., Girirajan, T. P., & Mason, M. D. (2006). Ultra-high resolution imaging by fluorescence photoactivation localization microscopy. *Biophysical Journal*, 91, 4258–4272. <https://doi.org/10.1529/biophysj.106.091116>
- Huisken, J., Swoger, J., Del Bene, F., Wittbrodt, J., & Stelzer, E. H. (2004). Optical sectioning deep inside live embryos by selective plane illumination microscopy. *Science*, 305, 1007–1009. <https://doi.org/10.1126/science.1100035>
- Hummer, G., Fricke, F., & Heilemann, M. (2016). Model-independent counting of molecules in single-molecule localization microscopy. *Molecular Biology of the Cell*, 27, 3637–3644. <https://doi.org/10.1091/mbc.E16-07-0525>
- Hummert, J., Yserentant, K., Fink, T., Euchner, J., Ho, Y. X., Tashev, S. A., & Herten, D. P. (2021). Photobleaching step analysis for robust determination of protein complex stoichiometries. *Molecular Biology of the Cell*, 32, ar35. <https://doi.org/10.1091/mbc.E20-09-0568>
- Jung, S. R., Fujimoto, B. S., & Chiu, D. T. (2017). Quantitative microscopy based on single-molecule fluorescence. *Current Opinion in Chemical Biology*, 39, 64–73. <https://doi.org/10.1016/j.cbpa.2017.06.004>
- Jungmann, R., Avendaño, M. S., Dai, M., Woehrstein, J. B., Agasti, S. S., Feiger, Z., Rodal, A., & Yin, P. (2016). Quantitative super-resolution imaging with qPAINT. *Nature Methods*, 13, 439–442. <https://doi.org/10.1038/nmeth.3804>
- Jungmann, R., Steinhauer, C., Scheible, M., Kuzyk, A., Tinnefeld, P., & Simmel, F. C. (2010). Single-molecule kinetics and super-resolution microscopy by fluorescence imaging of transient binding on DNA origami. *Nano Letters*, 10, 4756–4761. <https://doi.org/10.1021/nl103427w>
- Ke, Y., Ong, L. L., Shih, W. M., & Yin, P. (2012). Three-dimensional structures self-assembled from DNA bricks. *Science*, 338, 1177–1183. <https://doi.org/10.1126/science.1227268>
- Khater, I. M., Nabi, I. R., & Hamarneh, G. (2020). A review of super-resolution single-molecule localization microscopy cluster analysis and quantification methods. *Patterns*, 1, 100038. <https://doi.org/10.1016/j.patter.2020.100038>
- Kikuchi, K., Adair, L. D., Lin, J., New, E. J., & Kaur, A. (2022). Photochemical mechanisms of fluorophores employed in single-molecule localization microscopy. *Angewandte Chemie (International Ed. in English)*, e202204745. <https://doi.org/10.1002/anie.202204745>
- Konopka, C. A., & Bednarek, S. Y. (2008). Variable-angle epifluorescence microscopy: A new way to look at protein dynamics in the plant cell cortex. *The Plant Journal: For Cell and Molecular Biology*, 53, 186–196. <https://doi.org/10.1111/j.1365-313X.2007.03306.x>
- Kosuta, T., Cullell-Dalmau, M., Cella Zanacchi, F., & Manzo, C. (2020). Bayesian analysis of data from segmented super-resolution images for quantifying protein clustering. *Physical Chemistry Chemical Physics: PCCP*, 22, 1107–1114. <https://doi.org/10.1039/c9cp05616e>
- Kufer, S. K., Puchner, E. M., Gump, H., Liedl, T., & Gaub, H. E. (2008). Single-molecule cut-and-paste surface assembly. *Science*, 319, 594–596. <https://doi.org/10.1126/science.1151424>
- Leake, M. C., Chandler, J. H., Wadhams, G. H., Bai, F., Berry, R. M., & Armitage, J. P. (2006). Stoichiometry and turnover in single, functioning membrane protein complexes. *Nature*, 443, 355–358. <https://doi.org/10.1038/nature05135>
- Lelek, M., Gyparaki, M. T., Beliu, G., Schueder, F., Griffié, J., Manley, S., Jungmann, R., Sauer, M., Lakadamyali, M., & Zimmer, C. (2021). Single-molecule localization microscopy. *Nature Reviews Methods Primers*, 1, 39. <https://doi.org/10.1038/s43586-021-00038-x>
- Levet, F., Julien, G., Galland, R., Butler, C., Beghin, A., Chazeau, A., Hoess, P., Ries, J., Giannone, G., & Sibarita, J. B. (2019). A tessellation-based colocalization analysis approach for single-molecule localization microscopy. *Nature Communications*, 10, 2379. <https://doi.org/10.1038/s41467-019-10007-4>
- Li, H., & Yang, H. (2019). Statistical learning of discrete states in time series. *The Journal of Physical Chemistry B*, 123, 689–701. <https://doi.org/10.1021/acs.jpcc.8b10561>
- Magrassi, R., Scalisi, S., & Cella Zanacchi, F. (2019). Single-molecule localization to study cytoskeletal structures, membrane complexes, and mechanosensors. *Biophysical Reviews*, 11, 745–756. <https://doi.org/10.1007/s12551-019-00595-2>
- Milstein, J. N., Nino, D. F., Zhou, X., & Gradinaru, C. C. (2022). Single-molecule counting applied to the study of GPCR oligomerization. *Biophysical Journal*, 121, 3175–3187. <https://doi.org/10.1016/j.bpj.2022.07.034>
- Möckl, L., & Moerner, W. E. (2020). Super-resolution microscopy with single molecules in biology and beyond – Essentials, current trends, and future challenges. *Journal of the American Chemical Society*, 142, 17828–17844. <https://doi.org/10.1021/jacs.0c08178>
- Möller, J., Isbilir, A., Sungkaworn, T., Osberg, B., Karathanasis, C., Sunkara, V., Grushevskiy, E. O., Bock, A., Annibale, P., Heilemann, M., Schütte, C., & Lohse, M. J. (2020). Single-molecule analysis reveals agonist-specific dimer formation of μ -opioid receptors. *Nature Chemical Biology*, 16, 946–954. <https://doi.org/10.1038/s41589-020-0566-1>
- Moore, R. P., & Legant, W. R. (2018). Improving probes for super-resolution. *Nature Methods*, 15, 659–660. <https://doi.org/10.1038/s41592-018-0120-1>
- Mortensen, K. I., Churchman, L. S., Spudich, J. A., & Flyvbjerg, H. (2010). Optimized localization analysis for single-molecule tracking and super-resolution microscopy. *Nature Methods*, 7, 377–381.
- Nakajo, K., Ulbrich, M. H., Kubo, Y., & Isacoff, E. Y. (2010). Stoichiometry of the KCNQ1–KCNE1 ion channel complex. *Proceedings of the National Academy of Sciences of the United States of America*, 107, 18862–18867. <https://doi.org/10.1073/pnas.1010354107>
- . (2018). Method of the year 2017: Organoids. *Nature Methods*, 15, 1. <https://doi.org/10.1038/nmeth.4575>
- Nicovich, P. R., Owen, D. M., & Gaus, K. (2017). Turning single-molecule localization microscopy into a quantitative bioanalytical tool. *Nature Protocols*, 12, 453–460. <https://doi.org/10.1038/nprot.2016.166>
- Ostersehl, L. M., Jans, D. C., Wittek, A., Keller-Findeisen, J., Inamdar, K., Sahl, S. J., Hell, S. W., & Jakobs, S. (2022). DNA-PAINT MINFLUX nanoscopy. *Nature Methods*, 19, 1072–1075. <https://doi.org/10.1038/s41592-022-01577-1>
- Owen, D. M., Rentero, C., Rossy, J., Magenau, A., Williamson, D., Rodriguez, M., & Gaus, K. (2010). PALM imaging and cluster analysis of protein heterogeneity at the cell surface. *Journal of Biophotonics*, 3, 446–454. <https://doi.org/10.1002/jbio.200900089>
- Pennacchietti, F., Vascon, S., Nieuws, T., Rosillo, C., Das, S., Tyagarajan, S. K., Diaspro, A., del Bue, A., Petrini, E. M., Barberis, A., & Cella Zanacchi, F. (2017). Nanoscale molecular reorganization of the inhibitory postsynaptic density is a determinant of GABAergic synaptic potentiation. *Journal of Neuroscience*, 37, 1747–1756. <https://doi.org/10.1523/JNEUROSCI.0514-16.2016>
- Ripley, B. D. (1977). Modelling spatial patterns. *Journal of the Royal Statistical Society: Series B (Methodological)*, 39, 172–192. <https://doi.org/10.1111/j.2517-6161.1977.tb01615.x>
- Rust, M. J., Bates, M., & Zhuang, X. (2006). Sub-diffraction-limit imaging by stochastic optical reconstruction microscopy (STORM). *Nature Methods*, 3, 793–795.

- Sander, J. D., & Joung, J. K. (2014). CRISPR-Cas systems for editing, regulating and targeting genomes. *Nature Biotechnology*, 32, 347–355. <https://doi.org/10.1038/nbt.2842>
- Scalisi, S., Pennacchietti, F., Keshavan, S., Derr, N. D., Diaspro, A., Pisignano, D., Pierzynska-Mach, A., Dante, S., & Cella Zancchi, F. (2021). Quantitative super-resolution microscopy to assess adhesion of neuronal cells on single-layer graphene substrates. *Membranes*, 11, 878.
- Scheckenbach, M., Bauer, J., Zähringer, J., Selbach, F., & Tinnefeld, P. (2020). DNA origami nanorulers and emerging reference structures. *APL Materials*, 8, 110902. <https://doi.org/10.1063/5.0022885>
- Schnitzbauer, J., Strauss, M. T., Schlichthaerle, T., Schueder, F., & Jungmann, R. (2017). Super-resolution microscopy with DNA-PAINT. *Nature Protocols*, 12, 1198–1228. <https://doi.org/10.1038/nprot.2017.024>
- Sengupta, P., Jovanovic-Talman, T., Skoko, D., Renz, M., Veatch, S. L., & Lippincott-Schwartz, J. (2011). Probing protein heterogeneity in the plasma membrane using PALM and pair correlation analysis. *Nature Methods*, 8, 969–975. <https://doi.org/10.1038/nmeth.1704>
- Sengupta, P., & Lippincott-Schwartz, J. (2012). Quantitative analysis of photoactivated localization microscopy (PALM) datasets using pair-correlation analysis. *BioEssays*, 34, 396–405. <https://doi.org/10.1002/bies.201200022>
- Sharonov, A., & Hochstrasser, R. M. (2006). Wide-field subdiffraction imaging by accumulated binding of diffusing probes. *Proceedings of the National Academy of Sciences*, 103, 18911–18916. <https://doi.org/10.1073/pnas.0609643104>
- Shroff, H. et al. (2007) Dual-color superresolution imaging of genetically expressed probes within individual adhesion complexes. *Proceedings of the National Academy of Sciences of the United States of America*, 104, 20308–20313. <https://doi.org/10.1073/pnas.071051710>
- Siddig, S., & Aufmkolk, S. (2020). Super-resolution imaging reveals the nanoscale organization of metabotropic glutamate receptors at presynaptic active zones. *Science Advances*, 6, eaay7193. <https://doi.org/10.1126/sciadv.aay7193>
- Sigal, Y. M., Zhou, R., & Zhuang, X. (2018). Visualizing and discovering cellular structures with super-resolution microscopy. *Science*, 361, 880–887. <https://doi.org/10.1126/science.aau1044>
- Thevathasan, J. V., Kahnwald, M., Cieřliński, K., Hoess, P., Peneti, S. K., Reitberger, M., Heid, D., Kasuba, K. C., Hoerner, S. J., Li, Y., Wu, Y. L., Mund, M., Matti, U., Pereira, P. M., Henriques, R., Nijmeijer, B., Kueblbeck, M., Sabinina, V. J., Ellenberg, J., & Ries, J. (2019). Nuclear pores as versatile reference standards for quantitative superresolution microscopy. *Nature Methods*, 16, 1045–1053. <https://doi.org/10.1038/s41592-019-0574-9>
- Thompson, M. A., Lew, M. D., Badieirostami, M., & Moerner, W. E. (2010). Localizing and tracking single nanoscale emitters in three dimensions with high spatiotemporal resolution using a double-helix point spread function. *Nano Letters*, 10, 211–218.
- Thompson, R. E., Larson, D. R., & Webb, W. W. (2002). Precise nanometer localization analysis for individual fluorescent probes. *Biophysical Journal*, 82, 2775–2783.
- Tokunaga, M., Imamoto, N., & Sakata-Sogawa, K. (2008). Highly inclined thin illumination enables clear single-molecule imaging in cells. *Nature Methods*, 5, 159–161.
- Tsekouras, K., Custer, T. C., Jashnsaz, H., Walter, N. G., & Pressé, S. (2016). A novel method to accurately locate and count large numbers of steps by photobleaching. *Molecular Biology of the Cell*, 27, 3601–3615. <https://doi.org/10.1091/mbc.E16-06-0404>
- Ulbrich, M. H., & Isacoff, E. Y. (2007). Subunit counting in membrane-bound proteins. *Nature Methods*, 4, 319–321. <https://doi.org/10.1038/nmeth1024>
- Unterauer, E. M., & Jungmann, R. (2021). Quantitative imaging with DNA-PAINT for applications in synaptic neuroscience. *Frontiers in Synaptic Neuroscience*, 13, 798267. <https://doi.org/10.3389/fnsyn.2021.798267>
- van de Linde, S., Löschberger, A., Klein, T., Heidbreder, M., Wolter, S., Heilemann, M., & Sauer, M. (2011). Direct stochastic optical reconstruction microscopy with standard fluorescent probes. *Nature Protocols*, 6, 991–1009. <https://doi.org/10.1038/nprot.2011.336>
- Vogelsang, J., Steinhauer, C., Forthmann, C., Stein, I. H., Person-Skegro, B., Cordes, T., & Tinnefeld, P. (2010). Make them blink: Probes for super-resolution microscopy. *ChemPhysChem*, 11, 2475–2490. <https://doi.org/10.1002/cphc.201000189>
- Wu, Y.-L., Tschanz, A., Krupnik, L., & Ries, J. (2020). Quantitative data analysis in single-molecule localization microscopy. *Trends in Cell Biology*, 30, 837–851. <https://doi.org/10.1016/j.tcb.2020.07.005>

How to cite this article: Scalisi, S., Pisignano, D., & Cella Zancchi, F. (2023). Single-molecule localization microscopy goes quantitative. *Microscopy Research and Technique*, 86(4), 494–504. <https://doi.org/10.1002/jemt.24281>